Appl. Phys. B 71, 169–175 (2000) / Digital Object Identifier (DOI) 10.1007/s003400000285

Applied Physics B
Lasers
and Optics

Plasma-based nitrogen tail pulse shutter for CO_2-TEA lidar dial systems

T. Gasmi[1], H.A. Zeaiter[2], G. Ropero[1], A. González Ureña[1,*]

[1] Unidad de láseres y Haces Moleculares, Instituto Pluridisciplinar, Universidad Complutense de Madrid, Paseo Juan XXIII, 1, 28040 Madrid, Spain (E-mail: laseres@eucmax.sim.ucm.es)
[2] Universidad Alfonso X El Sabio, Departamento de Física, Madrid, Spain

Received: 27 December 1999/Revised version: 11 February 2000/Published online: 27 April 2000 – © Springer-Verlag 2000

Abstract. This paper presents the construction, use and characterisation of a laser-induced sealed plasma shutter to clip off the nitrogen pulse tail of a CO_2-TEA laser-based lidar dial system. Investigation of the optimum gas filling pressure, temporal profile of the clipped pulse, and the laser threshold power intensities to achieve ionisation growth and breakdown in helium, argon, and nitrogen are also presented. Values of these power density thresholds lie between 3×10^{11} W cm^{-2}–5×10^{12} W cm^{-2}, 2×10^{11} W cm^{-2}–2×10^{12} W cm^{-2} and 3×10^{13} W cm^{-2}–2×10^{14} W cm^{-2} for helium, argon, and nitrogen, respectively. The range resolution attainable with the present clipped pulses is 15 m, which is 30 times better than that readily obtained with the nitrogen-tailed pulses. Field measurements of the lidar returns with the clipped pulse from a co-operative target are presented.

PACS: 42.68.Wt; 52.75. Kq

In the Lidar laboratory of our Institute, we have developed a differential absorption Lidar-Dial station. The system is well known to be extremely useful for remote sensing and quantitative measurement of gaseous trace constituents of the lower atmosphere. Moreover, because of the fact that the output radiation from a CO_2 laser lies in the middle of the 8 to 12 μm atmospheric window, CO_2-laser-based dial systems have been applied to a wide range of remote sensing problems over the past 20 years [1, 2]. Lidar-dial systems operating in the infrared have been used for monitoring the presence of major atmospheric constituents such as CO [3, 4], NO [5], SO_2 [6], ozone [7], and others [8]. However, most of the recently reported studies have dealt solely, either directly or indirectly, with improvements of the accuracy of dial systems [9]. The experimental work has generally involved the analysis of large data sets, which yielded statistically useful results, but little technological information was obtained that would be useful for the design of more compact lidar systems with optimized sensitivity.

*Corresponding author.

The most dominant time constant attributed to CO_2-TEA laser pulses is its nitrogen tail that can extend for several microseconds beyond the gain-switched spike. If there is some low level of near-field scatter into the receiver, this effect can be quite significant, as the aerosol backscatter return is of the order of 10^{-4} of the transmitted power within this wavelength interval [10]. In this case, the unclipped, near-field scattered signal, which is seen at the receiver several μs after the peak laser pulse is transmitted, can interfere with the weak signal backscattered from the atmospheric aerosols. The latter is lying only hundreds of metres away from the lidar system, thus appearing coincident in time with the near-field scatter. This type of pulse limits the range resolution of lidars to some hundreds of metres unless pulse-deconvolution techniques [11] are adopted.

Short laser pulses can also be obtained by various techniques such as mode locking, free induction decay, pulse slicing with electro-optic switched [12–15]. However, output pulses from these require further amplification for any useful application due to their very low energy content. This problem is circumvented in this work by the use of a sealed plasma shutter [16] that achieves high range-resolved remote sensing of the urban pollution in the atmosphere.

The gas, which is normally insulating and transparent to the radiation at ordinary intensities, is rapidly transformed into highly conducting, self-luminous, hot plasma by the action of a high-intensity laser pulse. The resultant plasma interacts with the excitation pulse and modifies its temporal profile. The properties of the gaseous plasma created by focusing laser radiation have also been extensively studied since the first report of the laser-induced breakdown of air in 1963 [17–19].

Of course, electro-optic crystals such as CdTe and CdSe could be used between crossed polarisers to achieve the same results [20]. However, the minimum permissible clear aperture due to the large laser beam diameter is approximately 9 to 30 cm^2, requiring an excessively large and expensive electro-optic crystal; telescopic reduction of the beam diameter could be performed to reduce the required aperture at the expense of the beam divergence. It also possible to reduce the nitrogen tail by the use of a low-nitrogen laser gas mixture. However,

this approach reduces the energy in the gain-switched spike and does not eliminate the tail as fully as clipping does [21].

To our knowledge, most of the published work dealt mainly with the mechanisms of generating the plasma breakdown and its use as a retro-pulse isolator for high-power infrared lasers or as laser pulse clipper for IR multiphoton selective dissociation [22–26]. However, as far as CO_2-TEA laser-based lidars are concerned, the data [27] are still scarce. Dedicated investigation to the use of simple and rugged plasma shutters as devices for short pulse generation and hence as a means to provide laser pulses for range-resolved monitoring still needs to be provided. Moreover, intra-cavity and electrical discharge assisted plasma shutters showed their limitations in terms of complete clipping of the nitrogen tail. This behaviour is even pronounced in the case of shorter (~ 30 ns) pulses where shuttering of a N_2-rich mixture at short delays often resulted in a re-lighting of the optical pulse due to the excess vibrational energy stored in the N_2 molecules.

Although passive plasma shutters have been quite useful in practical CO_2 lasers, little has been reported about a detailed characterisation of the plasma shutter nor the criteria necessary to design it for a lidar application.

In the following paragraphs, we present the plasma cell-based experimental set-up and a detailed description of the main elements that were used in monitoring the laser-induced plasma parameters under investigation. The variation of the threshold intensities for gas breakdown as a function of the filling pressure for helium, argon, and nitrogen will be presented and analysed. The temporal evolution of the clipped pulse width with respect to gas pressure within the cell will be depicted and discussed. We conclude this article by reviewing the main results.

1 Experimental apparatus

The CO_2 laser lidar dial system operates with the general specifications listed in Table 1. It is designed and built as a system for detecting and mapping with high-resolution urban pollution and chemical vapour plumes. The sealed plasma-shutter pulse clipper, filled with gas, is shown in Fig. 1. The cell is located at the exit of the laser and is prior to the optics used to sample out the transmitted power. The collimated laser beam enters the afocal lens pair and is focused at a point in space producing an intensity that is to the level required for causing gas breakdown and creating plasma. The laser pulse provides therefore the means to initiate the breakdown at any desirable laser energy. The need for a higher breakdown level [28] and a long-term stability operation of the shutter dictated the choice of helium, argon, and nitrogen as filling gases.

The CO_2-TEA laser used in the present study, is a Lumonics 370 TS upgraded to operate at a repetition rate of 10 Hz, delivers up to 4.5 joule per pulse. A plano-convex ZnSe meniscus lens having a focal length of 100 mm is used to focus the laser beam whereas a second lens with the same specifications re-collimates the clipped outgoing beam. The aluminium cell, closed by two anti-reflection-coated ZnSe windows, was evacuated to a pressure better than 10^{-3} Torr and purged several times before filling any gas into the chamber. Measurement of breakdown thresholds of helium, argon, and nitrogen gases were carried out for static pressure of these gases in the range of 75 to 1500 Torr. This range of pressures was investigated during this work because the study was limited essentially to locating precisely and optimising the pressures at which the plasma effectively clips the nitrogen tail of the laser pulse. Laser energy was adjusted by varying the voltage of the laser modulator. A typical record of the beam profile at 10.6 μm and 9.5 μm is shown in Fig. 2. An energy meter (Gentec-ED500) was used to measure the energy of the laser. To examine the clipping efficiency, a room-temperature fast photon-drag with bandwidth of excess of 200 MHz was used to observe a small fraction of the laser beam that was scattered off a carbon block after transmission through the clipper assembly. The jitter in time for the clipping was approximately ± 10 ns and was set by the resolution of the digital generator used to initiate the laser fire. The divergence of the laser beam was less than 3 mrad. The waist diameters of the focused laser beams were measured by passing the razor-blade edge through the laser focus. The razor edge was mounted on a translation stage with micrometer positioning adjusters. The estimated area of the focal spot at 9 to 11 μm ranged from 3×10^{-12} cm^2 to 8×10^{-12} cm^2.

Table 1. Typical characteristics and performances of the CO_2-TEA lidar dial

Parameters	Specifications
Transmitter	
Laser	Tunable, pulsed CO_2-TEA Lumonics 370XT upgraded at 10 Hz
Pulse width	Unclipped pulse: 3.5 μs Clipped with plasma shutter: < 70 ns
Energy	1.2 J (gain-switched spike at P20)
Repetition rate	2–10 Hz
Wavelength	9.2 to 10.8 μm
Tuning	Scanner computer controlled
Receiver module	
Telescope	Newtonian 1830, F#/4.5
Field of view	5 mrad
Detector	EG&G LN-cooled: J15-D12
Data acquisition	
Computer	PC 200 MHz, 32 Mb RAM
Software language	C++
Digitization	Tektronix TDS 540–200 MHz, 8 bits
Interfaces	IEEE-488

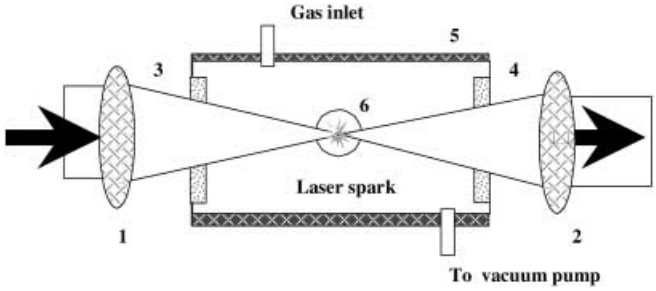

Fig. 1. Schematic of the sealed plasma shutter, 100-mm focal length ZnSe meniscus lens (1,2), AR coated ZnSe window (3,4), plasma chamber (5), visualisation window (6)

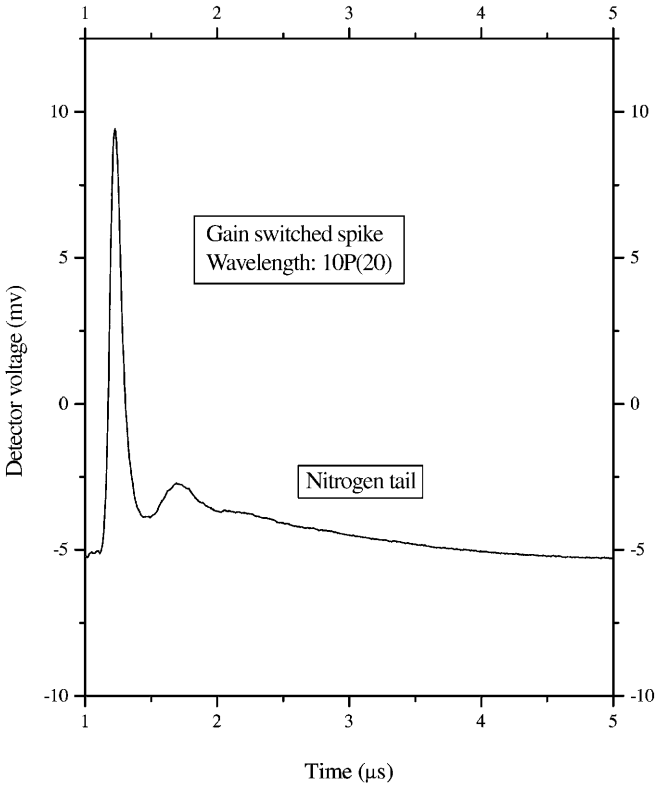

Fig. 2. Temporal profile of the unclipped CO_2-TEA laser pulse. The nitrogen pulse tail appears 1 μs after the gain switched spike and extends over 3 μs

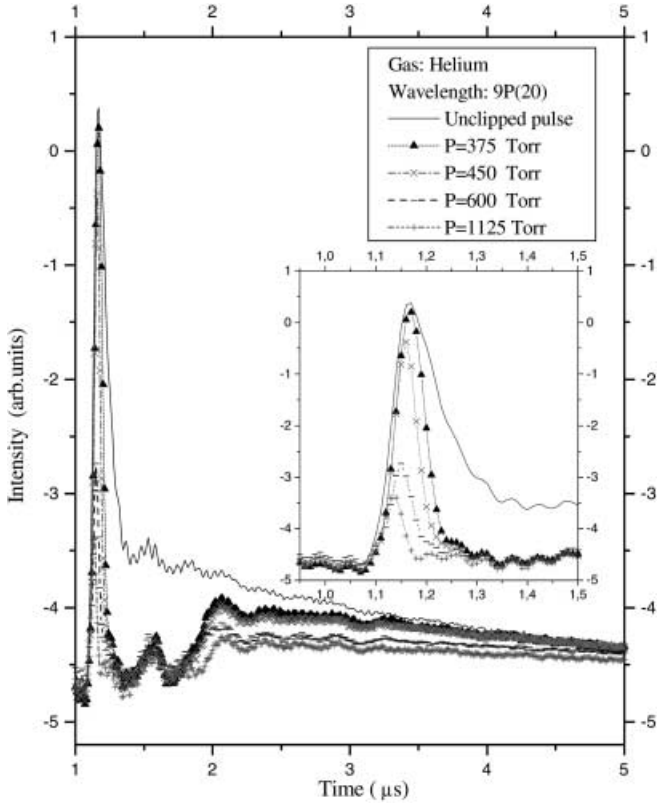

Fig. 3. Temporal profiles of the clipped laser pulse in the presence of helium as a function of the cell pressure. The pulse width decreases as the pressure in the cell is increased. The inset graph represents a magnified view of the clipped pulses during the first 500 ns interval

The optimum gas pressure that gave both the sharpest pulse cut and the highest efficiency in terms of minimum energy loss was obtained by varying the pressure of the cell while maintaining the laser input energy constant. To determine the breakdown threshold, the laser power was gradually increased while keeping the gas pressure in the cell fixed, until a visible spark, seen visually through the side window, was observed in the focal region.

2 Results and discussion

2.1 Temporal profile of the clipped pulse

An example of laser-induced clipping in helium is shown in Fig. 3. For the sake of clarity, each figure was limited to five curves to illustrate the evolution of the temporal profile of the clipped pulse as a function of pressure. The laser lines, used in this study, were mainly the 9P(20) and the 10P(20). However, all the other lines were clipped with equal facility, including the 9P(44). Careful examination of the baseline reveals that the attenuation of the clipped portion of the laser pulse within 500 ns of the breakdown is approximately 10^2; the degree of attenuation is somewhat sensitive to optical alignment. Some 2 to 3 μs after breakdown, a small recovery occurs and the attenuation factor drops to 10^1. The energy lost within the cell after clipping never exceeded 25%. The average clipping efficiency for helium at pressures of 600–900 Torr was approximately equal to 75%. This range of pressures achieved both the best attenuation of the nitrogen tail and best stability in terms of the transmitted energy. The efficiency, achieved with helium in this work, is superior than that reported by Parthasarathy [24] for a range of pressures extending from 200 to 300 Torr. Still, any further increase in the pressure would result in a progressive reduction of the efficiency.

Figure 4 shows the temporal profile of the clipped laser pulse as a function of pressure in the presence of nitrogen. Complete extinction of the nitrogen tail is achieved for pressures extending from 375 up to 1500 Torr. It should be noted, however, that increasing the gas pressure does indeed reduce the pulse width of the clipped pulse, but at the expense of the available laser energy that is recovered after clipping. Again careful examination of the baseline reveals that the attenuation of the clipped portion of the laser pulse is approximately 10^5, which is one order of magnitude higher than that already achieved with helium. No pulse recovery occurs after clipping takes place and the extinction factor maintains the same value throughout the duration of the original CO_2-TEA laser pulse. Nevertheless, the plasma clipping action drains out almost 40% of the laser energy. This energy loss is relatively high but is still acceptable considering the multi-joule energy output that a CO_2-TEA laser can deliver.

The temporal profile of the clipped laser pulse with argon as a filling gas in the cell is depicted in Fig. 5. No pulse recovery is observed after clipping is initiated. The argon plasma was both stable and repetitive all along the pressure interval from 150 to 1500 Torr. During the whole duration of the ni-

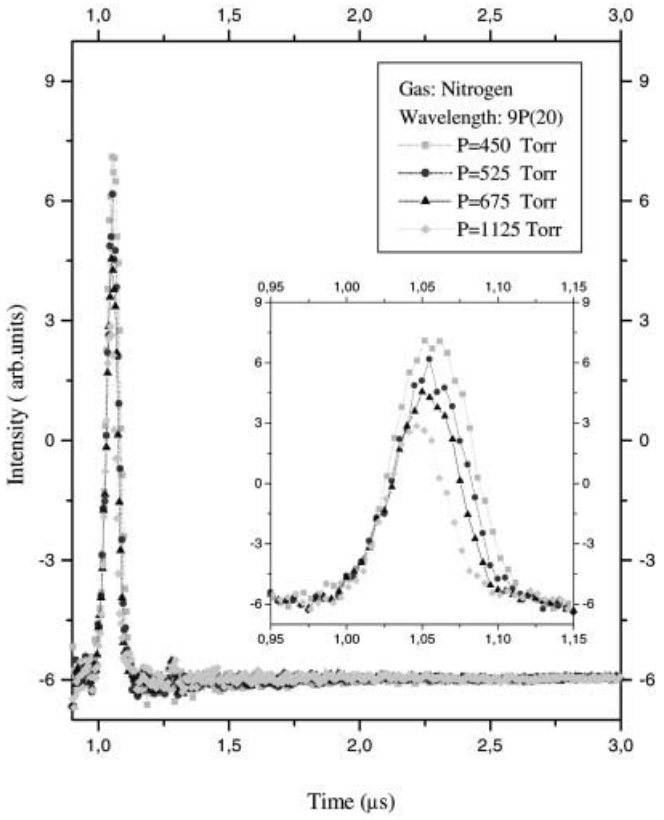

Fig. 4. Temporal evolution of the clipped laser pulses in presence of nitrogen at the various indicated pressures. No pulse recovery is observed after clipping of the pulse. The inset graph depicts the reduction in the laser pulse width as the pressure within the cell is increased

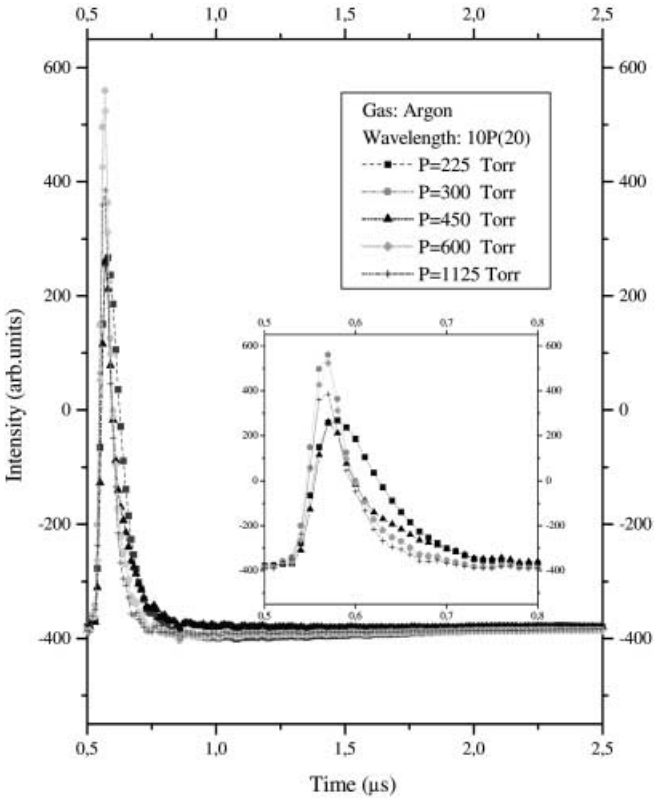

Fig. 5. Temporal profiles of the clipped laser pulse in the presence of argon as a function of pressure. Notice the pulse width reduction and the complete extinction of the nitrogen tail after clipping

trogen tail the attenuation of the clipped portion of the laser pulse is approximately 10^5. Again, the same observation was made with regards to the clipping efficiency in the presence of argon. More than 50% of the input energy is lost to the plasma upon clipping.

The evolution of the laser pulse width versus cell pressure for helium, argon, and nitrogen is illustrated in Fig. 6. A gradual change in the laser pulse width can be noticed as soon as the pressure for helium and nitrogen exceeds 300 Torr. Rapid decrease of the width of the clipped pulse is thereupon observed for a pressure range between 300–600 Torr. A nearly asymptotic value of the width is reached at pressures higher than 700 Torr. Further increase of the filling pressure of the three gases beyond this value does not affect the final trend of the laser pulse. For argon, however, once the breakdown is initiated within the cell, the evolution of the clipped pulse width versus time does not show any gradual transition from a nitrogen-tailed pulse to a clipped pulse even at pressures below 150 Torr. In other words, the clipping is effective as soon as the laser pulse is launched into the cell.

Figure 7 shows a typical round-trip return of the signal of the lidar pulse. The dotted curve depicts the return of the raw pulse of the lidar where the effect of the nitrogen-tail pulse is clearly identified by the presence of a second hump. The latter is delayed 1 μs after the arrival of the gain-switched spike. The solid-line curve is the return of the clipped pulse in the presence of helium, argon, and nitrogen. The detected signal clearly shows the normal exponential decay of the single gain-switched spike of the CO_2-TEA laser and a total absence

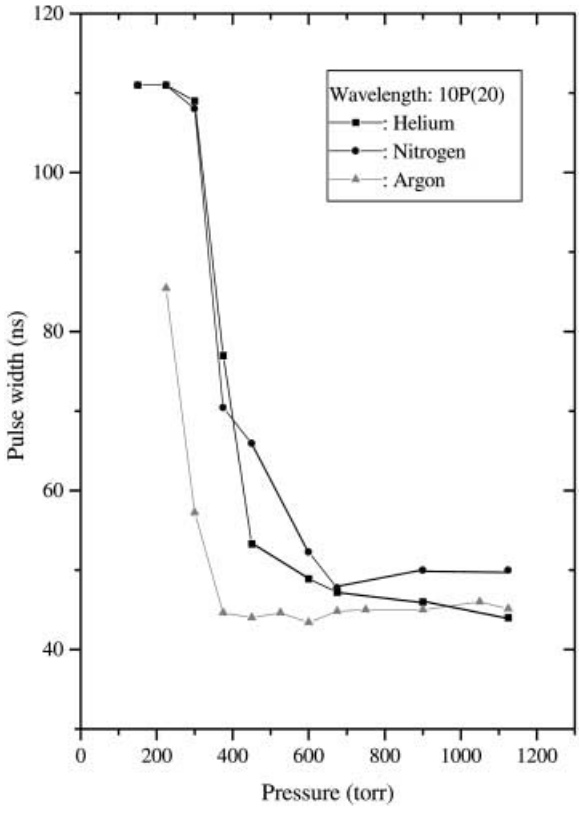

Fig. 6. Evolution in time of the clipped pulse width as a function of pressure for helium, nitrogen and argon

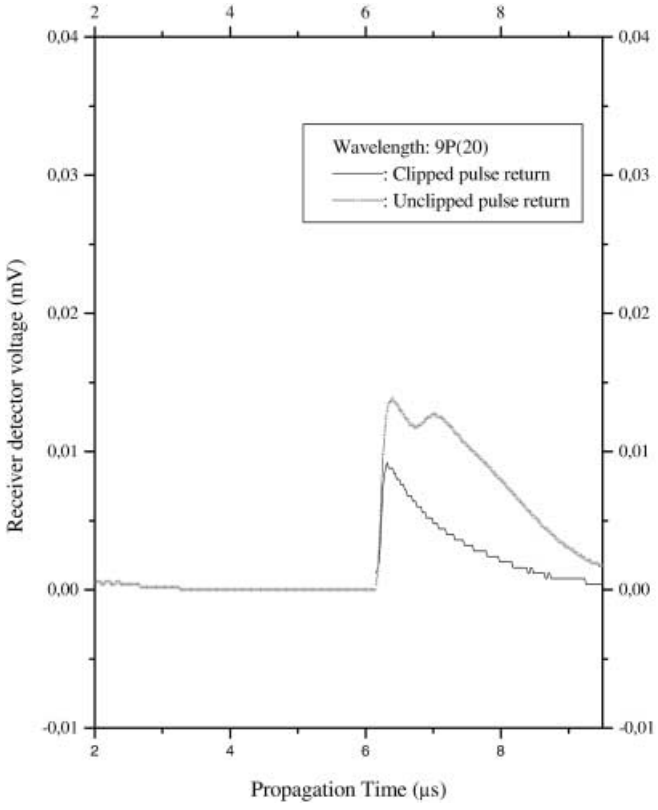

Fig. 7. Typical round trip return of the CO_2-TEA dial lidar. The signal of the clipped pulse follows the normal exponential decay time of the gain-switched spike while the unclipped pulse shows the second hump due to the nitrogen tail

of the hump, which was initially associated with the nitrogen tail of the CO_2-TEA pulse. Moreover, the pulse recovery observed for helium had no significant effect on the pulse return since its energy content was very low. The long exponential decay time is inherent to the EG&G J15-D12 detector whose time constant is approximately 400 ns. The difference in intensity between the two signals is mainly due to the power loss within the shutter upon clipping of the pulse.

2.2 Laser-breakdown threshold

Since the earliest observations of laser-induced breakdown in gases, much consideration has been given to the laser intensity required for breakdown [29]. The optical breakdown is a function of the gas pressure, the ionisation potential of the gas and the pulse width of the laser. In laser-induced dielectric breakdown, the extremely rapid transformation from neutral gas into hot gas plasma takes place in three distinct phases, (a) initiation, (b) formative growth and onset of breakdown, and (c) plasma formation accompanied by the generation of shocks and their propagation [18].

Two mechanisms are proposed for the initial ionisation. One involves ionisation by multiphoton absorption whereas the other involves cascade-ionisation-assisted collisions. As soon as conditions for the onset of breakdown are satisfied, ionisation growth will continue as long as the irradiation continues. There then follows the rapid plasma development stage with production of highly ionised hot expanding gas in which further laser light absorption, heating, and hydrodynamic processes become increasingly important. As the electron and ion concentrations increase both electron–ion and ion–ion interactions contribute to the growth mechanisms. The gas will remain heated for substantially longer than the duration of the laser pulse which created it, but the extinction processes of recombination, diffusion, radiation, and conduction remove energy from the plasma region, and local thermodynamic equilibrium with surrounding gas is established in about microsecond time scale. Thus, laser-induced dielectric breakdown acts like a switch which allows the leading edge of the excitation laser pulse to pass through the plasma cell as a short spike while absorbing and scattering [26] the remaining part of the incident light.

However, because very near the threshold the appearance of the spark could be quite erratic, the threshold was defined as the power setting for which the visible spark was ignited with nearly 10% probability. To check the reproducibility of the results, the experiments were repeated several times for all pressures at all wavelengths. Breakdown thresholds were estimated from the average of several pulses, nominally 1000 at 10 Hz.

Figure 8 shows the measured values of the threshold breakdown intensities as a function of pressure for helium, argon, and nitrogen over the pressure range of 75–1500 Torr. The 100 ns gain-switched pulse of the CO_2-TEA laser induces the gas breakdown. Since it is customary to express the pressure dependence of the intensity thresholds, I_{th}, by $I_{th}\alpha P^{\beta}$ ($\beta < 0$), the data for the 10(P20) line have been plotted on a $\log(I_{th})$ versus $\log(P)$ scale and fitted to a straight

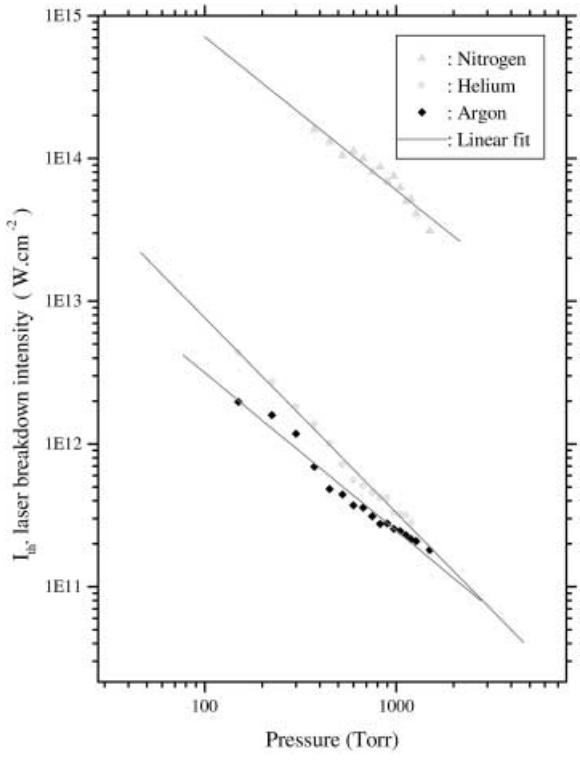

Fig. 8. Threshold breakdown intensities for nitrogen, helium and argon versus the cell pressure. The linear fitting of the data for the three gases shows a continuous line with a gradient of (−1.1) which supports the predominance of the collisional ionization mechanism in the three gases

line. The latter appears reasonable for most of the data sets, although some could perhaps be better interpreted as a two-slope fit. The scatter of points about the straight line gives an approximate measure of what we believe to be the uncertainty in our measurements: the standard deviations of the fits are 1%–8%. In reporting the results, we have lumped together the helium, argon, and nitrogen to obtain a larger database for comparison.

For helium, the pressure dependence of the breakdown threshold intensity is noticeable. The threshold intensities extend from $3 \times 10^{11}\,\mathrm{W\,cm^{-2}}$–$5 \times 10^{12}\,\mathrm{W\,cm^{-2}}$. There is no evidence for the plateau in the threshold curve of the kind observed and predicted by the multiphoton ionisation (MPI) processes in gases [30]. The curve shows, instead, a continuous line with a gradient of about (−1.1). This result agrees reasonably well with the work of Morgan et al. [31]. It also confirms the predominance of the collision ionisation process over the other mechanisms. The absence of this plateau is due to the IR emission band of CO_2-TEA lasers. At infrared wavelengths, laser-induced breakdown is generally understood to occur by an avalanche ionisation mechanism [32] in which the initial "seed" electrons are produced by MPI or thermal processes. However, at wavelengths less than 1 μm, laser-induced breakdown in a gas is believed to occur by way of MPI and collision/avalanche ionisation processes [33].

For argon, the breakdown threshold intensities lie well below that of helium and are also dependent on pressure over the range 75–1500 Torr. The argon curve also shows the same tendency observed with the helium. The threshold intensities stretch out from $2 \times 10^{11}\,\mathrm{W\,cm^{-2}}$–$2 \times 10^{12}\,\mathrm{W\,cm^{-2}}$.

For nitrogen, the curve shows a dependence of the threshold intensities on pressure for the whole pressure range under investigation. The threshold intensities extend from $3 \times 10^{13}\,\mathrm{W\,cm^{-2}}$–$2 \times 10^{14}\,\mathrm{W\,cm^{-2}}$. Very high stability and reproducibility of the breakdown are achieved only for the pressures above 375 Torr. The range of threshold intensities is rather higher than for helium and argon due to the additional vibrational energy losses inherent to the nitrogen molecule. The nitrogen molecule is usually considered as a five-level system [33].

So with the increase in gas pressure, the threshold for breakdown for the three gases under investigation, goes on decreasing leading to an earlier onset of the plasma formation. This results in a faster switching of the excitation pulse with a concomitant shortening of the transmitted pulse through the plasma cell. Energy efficiency for the output beam, however, gets progressively reduced because a larger part of the excitation pulse gets absorbed or scattered.

3 Conclusion

We presented the construction, characterisation and use of a laser-induced sealed plasma shutter to clip off the nitrogen pulse tail of a CO_2-TEA laser-based lidar dial system. Results on the optimum gas-filling pressure, temporal profile of the clipped pulse, and the laser threshold power densities to achieve ionisation growth and breakdown in helium, argon, and nitrogen are also reported. Few tens of ns clipped pulses with an attenuation ranging from 10^3–10^5 are achieved at power density thresholds lying between $3 \times 10^{11}\,\mathrm{W\,cm^{-2}}$–$5 \times 10^{12}\,\mathrm{W\,cm^{-2}}$, $2 \times 10^{11}\,\mathrm{W\,cm^{-2}}$–$2 \times 10^{12}\,\mathrm{W\,cm^{-2}}$ and $3 \times 10^{13}\,\mathrm{W\,cm^{-2}}$–$2 \times 10^{14}\,\mathrm{W\,cm^{-2}}$ for helium, argon, and nitrogen, respectively. The optimum pressures for the three gases, which provided the best operation stability of the transmitted energy and the highest attenuation of the nitrogen tail, are located within the 450–600 Torr interval. Complete extinction of the nitrogen tail is achieved for pressures extending from 375 to 1500 Torr for both nitrogen and argon gases. For helium, some 2 to 3 μs after breakdown, a small recovery occurs with no significant effect on the spatial resolution of the lidar-dial system. The range resolution attainable with the present clipped pulses is 15 m, which is 30 times better than that readily obtained with the nitrogen-tailed pulses. The average energy efficiency after clipping is 75% for the helium and 60% for argon and nitrogen. The shutter provides therefore pulses for high range-resolved remote sensing of atmospheric urban pollution with minimum laser power loss. Field measurements of the lidar returns with these clipped pulses, reflected off co-operative targets, confirmed the great improvement in the spatial resolution of the lidar-dial system.

A further possible application of this plasma shutter could be in the studies of non-linear phenomena where the effect of the high peak power spike can be obscured by those due to the significant energy present at lower intensities in the pulse tail.

The shutter is also characterised by its simplicity, ruggedness, reliability, and very low cost of construction.

Acknowledgements. Support by the Conserjería de Educación y Cultura of the Comunidad Autónoma de Madrid Grant No 07M/0390/1997 and DGES Grant PB97-0272 are gratefully acknowledged.

References

1. H. Ahlberg, S. Lunqvist, M.S. Shumate, U. Person: Appl. Opt. **24**, 3947 (1985)
2. D.K. Killinger, N. Menyuk: Appl. Phys. Lett. **38**, 968 (1981)
3. T. Henningsen: Appl. Phys. Lett. **24**, 242 (1974)
4. D.K. Killinger, N. Menyuk, W.E. De Feo: Appl. Phys. Lett. **36**, 402 (1980)
5. N. Menyuk, D.K. Killinger: Appl. Opt. 19 **9**, 3282 (1980)
6. R.A. Baumgartner, R.L. Byer: Opt. Lett. **2**, 163 (1978)
7. K. Asai, T. Itabe, T. Igarashi: Appl. Phys. Lett. **35**, 60 (1979)
8. E.R. Murray: Opt. Eng. **17**, 30 (1978)
9. H.V. Piltingsrud: Appl. Opt. **27**, 3952 (1991)
10. M.L. Wright, E.K. Protor, L.S. Gasiorek, M.L. Liston: NASA CR-132724 (1975)
11. Y. Zhao, T.K. Lea, R.M. Schotland: Appl. Opt. **27**, 2730 (1988)
12. A.W. Pasternak, D.J. James, J.A. Nilson, D.K. Evans, R.D. Mc Alpine, H.M. Adams, E.B. Selzirk: Appl. Opt. **20**, 3849 (1981)
13. E. Yablonovitch, J. Goldhar: Appl. Phys. Lett. **25**, 850 (1974)
14. M. Hasselbeck, L. Huang, S.C. Hsu, H.S. Kwok: Rev. Sci. Instrum. **54**, 1131 (1983)
15. M. Quack, C. Ruede, G. Seyfang: Spectrochim. Acta **46A**, 523 (1990)
16. J. Moser, P. Morand, R. Duprex, H. Van der Bergh: Chem. Phys. **79**, 277 (1983)
17. C.G. Morgan: *Electrical Breakdown of Gases* (Wiley, Chichester 1978)
18. T.P. Hughes: *Plasmas and Laser Light* (Adam Hilger, London 1975)
19. P. Laporte, N. Damany, H. Damany: Opt. Lett. **12**, 987 (1987)
20. M.S. Mangir, C.G. Parazzoli: Conference on lasers and electro-optics, Baltimore MD, Paper WO3 (1983)
21. P. Holland, J. Van der Laan, K. Phelps, S. Gotoff: Proceedings of the International Conference on Lasers 87, 694, (STC, McLean, Va 1988)
22. N.J. Burnet, M.C. Richardson: Rev. Sci. Instrum. **47**, 2 (1976)
23. H.S. Kwok, E. Yablonovitch: Opt. Commun. **21**, 252 (1977)
24. V. Parthasarathy, S. Nad, K. Rao, S.K. Sarkar: J. Photochem. Photobiol. A: Chem. **115**, 1 (1998)
25. J.F. Figueira, S.J. Czuchlewski, C.R. Phipps Jr., S.J. Thomas: Appl. Opt. **20**, 5 (1981)

26. T.A. Znotins, S.R. Byron, S.E. Moody, R.K. Brimacombe, J. Reid: Rev. Sci. Instrum. **55**, 6 (1984)
27. C.B. Carlisle, J.E. Van der Laan, L.W. Carr, P. Adams, J.P. Chiaroni: Appl. Opt. **34**, 27 (1995)
28. D.R. Lide: *Handbook of Chemistry and Physics*, 74th edn. (CRC Press, Boca Raton 1994)
29. R.J. Dewhurst: J. Phys. D **11**, 191 (1978)
30. C.L.M. Ireland, C.G. Morgan: J. Phys. D **6**, 720 (1973)
31. F. Morgan, J.R. Evans, C.G. Morgan: J. Phys. D **4**, 225 (1971)
32. R. Tambay, R.K. Thareja: J. Appl. Phys. **70**, 2890 (1991)
33. J.P. Davis, A.L. Smith, C. Giranda, M. Squicciarini: Appl. Opt. **30**, 5358 (1991)